

Original Article

Bone marrow mesenchymal stem cells-secreted exosomal H19 modulates lipopolysaccharides-stimulated microglial M1/M2 polarization and alleviates inflammation-mediated neurotoxicity

Lu Zong¹, Pu Huang¹, Qing Song¹, Yan Kang²

¹Department of Obstetrics, The First Affiliated Hospital of Xi'an Jiaotong University, Xi'an 710061, Shaanxi, China;

²Department of Obstetrics, Shandong Provincial Maternal and Child Health Care Hospital, Cheeloo College of Medicine, Shandong University, Ji'nan 250014, Shandong, China

Received September 1, 2020; Accepted December 26, 2020; Epub March 15, 2021; Published March 30, 2021

Abstract: Neuroinflammation is the most common cause of neurological diseases. Exosomes derived from mesenchymal stem cells (MSCs-exos) have been reported to reduce inflammation and neuronal injury. Its underlying mechanism remains poorly unknown. In this study, identification of bone marrow MSCs-derived exosomes (BMSCs-exos) was conducted by nanosight tracking analysis, transmission electron microscope, and western blot assay. Enzyme-linked immunosorbent (ELISA) was used to analyze microglial M1/M2 polarization and detect levels of inflammatory factors. Cell viability was determined by Cell Counting Kit (CCK)-8 assay. Cell apoptosis was assessed by flow cytometry, caspase-3 activity assay, and DNA fragmentation assay. Quantitative real-time polymerase chain reaction was used to detect gene expression. Luciferase reporter and RNA pull-down assays were exploited to validate the interaction between genes. BMSCs-exos promoted M2 polarization while inhibited M1 polarization in LPS-stimulated BV-2 cells. BMSCs-exos inhibited the secretion of interleukin (IL)-1 β , IL-6, and TNF- α , while increased the levels of IL-10. BMSCs-exos resisted the cytotoxicity and apoptosis induced by LPS in HT22 cells. BMSCs-exosomal long noncoding RNA (lncRNA) H19 enhanced the anti-inflammatory ability of BMSCs-exos in BV-2 microglia following LPS stimulation, and strengthened the neuroprotective effect of BMSCs-exos on HT22 cells in the presence of LPS. Moreover, H19 functioned as a sponge for miR-29b-3p. miR-29b-3p mimics abolished the effects of BMSCs-exosomal H19 on M1/M2 polarization and inflammation in LPS-stimulated BV-2 cells. The neuroprotective function of BMSCs-exosomal H19 was attenuated by miR-29b-3p mimics in LPS-stimulated HT22 cells. BMSCs-exosomal H19 modulates LPS-stimulated microglial M1/M2 polarization and alleviates inflammation-mediated neurotoxicity by sponging miR-29b-3p.

Keywords: Mesenchymal stem cells, exosomes, microglia, long non-coding RNA H19

Introduction

The substantial damage of intrauterine infection is mainly due to the inflammatory response, which is shared by various damages and disorders of the central nervous system [1]. Fetal inflammatory response syndrome (FIRS) caused by intrauterine infection during pregnancy is the most common reason of preterm and premature white matter damage (WMD), and is associated with subsequent neurological impairment of various severity (Including cerebral

palsy) [2]. Microglia, as the prime innate immune cells in the brain, are derived from the monocyte/macrophage lineage and act a key part in immune regulation and inflammation after brain injury [3]. It is well known that microglia are in a classic balance of pro-inflammatory (M1 phenotype) and anti-inflammatory (M2 phenotype). The phenotypic change of microglia is related to the local microenvironment [4]. Microglia can be induced to M1 polarization by lipopolysaccharide (LPS) or interferon γ , and also can be induced to M2 polarization by

interleukin (IL)-4, IL-10, and transforming growth factor α *in vitro* [5]. Therefore, the neuroinflammatory response can be repressed by adjusting the balance of the polarization of M1/M2, which is of great significance for protecting the nervous system from secondary damage [6].

So far, the transplantation of mesenchymal stem cells (MSCs) has been studied in the therapy of kinds of organ injuries due to its immunosuppressive and anti-inflammatory properties [7]. MSCs-based therapy can restore the structure and function of damaged tissues [8, 9]. MSCs-derived exosomes (MSCs-exos) are membrane-like structure derived from the cytoplasm, recognized by the enrichment of CD9, CD63, and CD81, which are specific markers from the transmembrane protein superfamily [10]. Exosomes have been shown to mediate communication between neurons and glia, promote neuronal repair and growth, and regulate immune responses [11, 12]. Recent studies have confirmed that MSCs-exos can effectively trigger the differentiation of macrophages from M1 to M2 phenotype [13]. Moreover, MSCs-exos can reduce inflammation and brain damage after ischemia-reperfusion injury [14].

Exosomes, as key regulators of cell-to-cell communication [15], mediate local cell communication by transferring coding RNA, noncoding RNA, DNA, and proteins [16]. A few long non-coding RNAs (lncRNAs) have been found to be enriched in exosomes and function as novel biomarkers and therapy targets in various diseases. For example, exosomal lncRNA-high expression in hepatocellular carcinoma can be used as a potential biomarker in hepatitis C virus infection-related hepatocellular carcinoma [17]. Exosomal lncRNA-urothelial carcinoma associated 1 may be used as a diagnostic biomarker in bladder cancer [18]. Mustafa et al. [19] showed that the monitoring of exosomal lncRNA-p21 may be used as a diagnostic indicator for evaluating the malignant state of prostate cancer patients. Chen et al. [21] showed that macrophage derived exosomal lncRNA growth arrest-specific 5 can enhance oxidized low density lipoprotein-induced apoptosis of vascular endothelial cells. Additionally, Liu et al. [22] showed that Krüppel-like factor 3 anti-sense RNA 1 derived from MSCs exosomes can inhibit the cartilage damage induced by IL-1 β stimulation. Up to now, it is not clear whether

MSCs-derived exosomal lncRNAs can be used as therapeutic targets for inflammation-induced nerve damage.

Lipopolysaccharide (LPS)-stimulated microglia BV-2 has been widely accepted as an *in vitro* model of neuroinflammation [23]. Herein, we investigated the anti-inflammatory function of BMSCs-derived exosomal H19 in LPS-induced mouse BV-2 microglia cells *in vitro*. Moreover, the protection of BMSCs-exos against neuroinflammation-induced neuronal injury in mouse hippocampal HT22 cells was further investigated. This study may produce a new insight into exosomal circulation lncRNAs during neuroinflammation.

Materials and methods

Cell culture and treatment

Mouse BMSCs were obtained from Cyagen Biosciences Inc. (Guangzhou, China). BMSCs were maintained in DMEM medium containing 10% FBS (growth media) or exos-depleted FBS (exosome derivation media), 100 U/mL penicillin and streptomycin, and incubated in a humid environment at 37°C and 5% CO₂. Passage 3-7 cells were used for subsequent experiments. In order to overexpress H19, the complete sequence of H19 was subcloned into the pcDNA3.1 vector to construct pcDNA-H19. Use empty pcDNA3.1 (pcDNA) as a control. pcDNA-H19 or pcDNA was transfected into BMSCs using Lipofectamine 2000 (Invitrogen, Carlsbad, CA, USA) in accordance with the user's instructions. After 48 h, the overexpression efficiency was checked by quantitative real-time polymerase chain reaction (qRT-PCR). As per the user's instructions, the total exosome isolation kit (Invitrogen) was used to isolate the corresponding exosomes from the supernatant of BMSCs and BMSCs transfected with pcDNA-H19 or pcDNA, including BMSCs-exos, pcDNA-H19-exos, and pcDNA-exos.

BV-2 microglia cells were purchased from CoBioer (Nanjing, China). BV-2 cells were incubated in DMEM (Gibco, Grand Island, NY, USA) with 10% FBS (growth media) or exos-depleted FBS (for experiment analysis) and 1% penicillin and streptomycin (Sigma-Aldrich, St. Louis, MO, USA) at 37°C in a incubator with 5% CO₂. To evaluate the effect of BMSCs-exos on LPS-stimulated BV-2 cells, BV-2 cells were exposed

MSCs-secreted exosomal H19 mitigates neuroinflammation

to the specified dose of LPS (1 $\mu\text{g}/\text{mL}$; Sigma-Aldrich) for 12 h and cultured with different concentrations (5, 10, and 20 $\mu\text{g}/\text{ml}$) of BMSCs-exos for 48 h. To confirm the anti-neuroinflammation effect of miR-29b-3p on BMSCs-exosomal H19, BV-2 cells transfected with miR-29b-3p mimic were cultured with exosomes derived from different BMSCs for 48 h. miR-29b-3p mimics and corresponding control were purchased from GenePharma (Shanghai, China).

Mouse hippocampal cells HT22 were obtained from Procell Life Science & Technology Co., Ltd. (CL-0595; Wuhan, China). HT22 cells were maintained in DMEM (Gibco) supplemented with 10% FBS (growth media) or exos-depleted FBS (for experiment analysis). To explore the exact mechanism of BMSCs-exosomal H19 in neuronal apoptosis induced by LPS, miR-29b-3p mimics were transfected into HT22 cells and then treated with LPS for 12 h (1 $\mu\text{g}/\text{mL}$) and pcDNA-H19-exos for 48 h.

Extraction and identification of BMSCs-derived exosomes

After cell transfection and incubation for 24 h in DMEM (Gibco) supplemented with 10% exos-depleted FBS, exos were isolated from the supernatant of BMSCs. Briefly, BMSCs conditioned medium was collected and centrifuged at 3000 g for 15 minutes at 4°C. The supernatant was incubated with 0.5 volume of total exosomes separation reagent (Invitrogen) at 4°C overnight. After centrifuging the mixture at 12000 g for 1 h, the precipitate was collected. The exosomes pellet was resuspended in 200 μl PBS for verification. The concentration and size distribution of BMSCs-exos were assessed by the Nanosight LM10 system (Nanosight, Amesbury, UK). The transmission electron microscopy (TEM) was applied to assess the morphological characteristics. The characteristic surface marker proteins of BMSCs-exos were determined by western blot assay.

Western blot assay

The concentration of total proteins extracted from cells or exosomes was measured with the BCA kit (Beyotime, Shanghai, China). Equal amounts (50 μg) of protein lysates were separated on 10% SDS-PAGE and then transferred onto PVDF membranes. Membranes were

blocked in 5% skim milk followed by incubation overnight at 4°C with anti-CD63, anti-CD9, or anti-CD81 antibody. Membranes were incubated with corresponding secondary antibody (Abcam) for 1 h at room temperature. After washing, the immunoblots were visualized with the enhanced chemiluminescence Western blotting substrate (ThermoFisher, San Jose, CA, USA).

Cell Counting Kit (CCK)-8 assay

As per the user's instructions, the cell viability was detected using the CCK-8 kit (Beyotime). Briefly, BV-2 cells were planted in the 96-well plates (2×10^3 cells/well) and cultured at 37°C under 5% CO_2 /95% air overnight. After rinsing with PBS, HT22 cells are exposed to LPS combined with or without exosomes derived from different BMSCs. After 48 h of treatment, 10 μl of CCK-8 was supplemented to each well and cultured at 37°C for 3 h. The optical density (OD) value was detected at 450 nm wavelength plate.

qRT-PCR

TRIzol kit (Invitrogen) was used to pick up total RNA from cells or exosomes. The iScript cDNA synthesis kit (Bio-Rad, China) was used to reverse transcribe RNA into cDNA. qRT-PCR was performed using the SYBR Premix Ex Taq™ kit (TaKaRa). The $2^{-\Delta\Delta\text{Ct}}$ method was used to determine the relative gene expression level.

Enzyme-linked immunosorbent (ELISA) assay

The contents of IL-1 β , IL-6, TNF- α , and IL-10 released in the conditioned medium were evaluated according to the specific ELISA kits (Beyotime) according to the manufacturer's protocol.

A commercially ELISA kit (Roche Applied Science, Penzberg, Germany) was utilized to evaluate the cellular DNA fragmentation in HT22 cells as per the manufacturer's protocol. The OD value at 450 nm was detected and expressed as the level of DNA fragmentation.

Caspase-3 activity

Apoptosis was evaluated according to the caspase-3 activity assay kit (Beyotime). In brief, cells were collected and lysed using RIPA buf-

MSCs-secreted exosomal H19 mitigates neuroinflammation

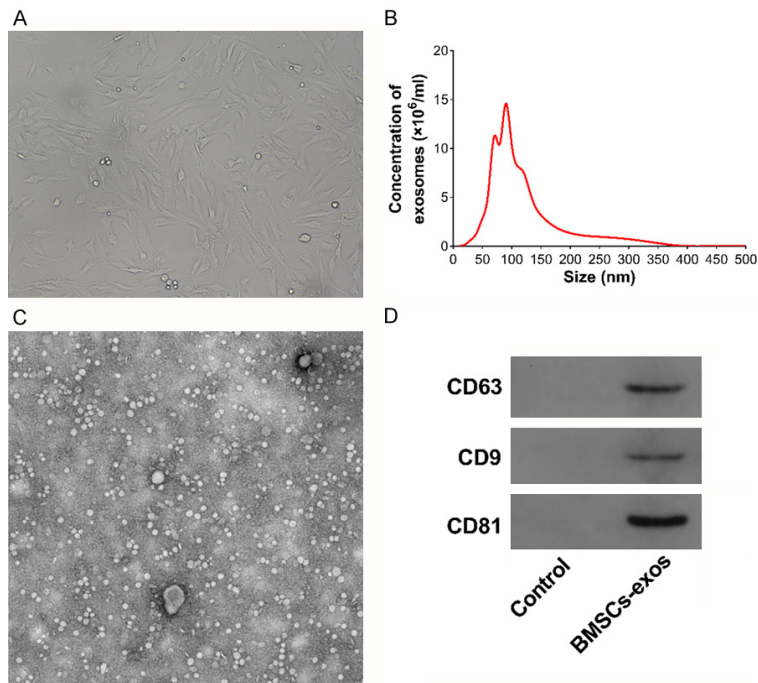


Figure 1. Morphological observation of BMSCs and identification of BMSCs-exos. A. The morphology of BMSCs was observed using phase morphology. B. The diameter of exosomes was detected by Nanosight tracking analysis. C. Transmission electron microscope was used to observe the morphology of MSCs-derived exosomes (MSCs-exos). D. The expression of CD63, CD9, and CD81 on the surface of exosomes was detected by Western blot.

fer. Reagents were added according to the manufacturer's recommendation, and the activity of caspase-3 was calculated by measuring the OD value at 450 nm.

Cell apoptosis assay

Annexin V and propidium iodide (PI) apoptosis assay kit (Beyotime) was applied to analyze the apoptosis rate of HT22 cells treated as indicated. After washing three times with PBS, HT22 cells were stained with Annexin V (5 μ l) and PI (5 μ l) for 20 min at room temperature in the dark. The percentage of apoptotic cells was then analyzed by flow cytometry (BD Biosciences, San Jose, CA, USA).

Luciferase reporter assay

The fragment of lncRNA H19 containing the predicted wild-type (WT) or mutant (MUT) binding sites were amplified and subcloned into the priCHECK2 vector (Promega, Madison, USA), named H19-WT and H19-MUT. Luciferase plasmid and miR-29b-3p mimics or miR-NC were

co-transfected into BV-2 cells using Lipofectamine 2000 (Invitrogen). At 48 h after transfection, luciferase activity was analyzed using a luciferase reporter assay system (Promega).

RNA pull-down

BV-2 cells were lysed using RIPA lysis buffer (Beyotime). Followed by the lysate was incubated with 3 μ g of biotinylated miR-29b-3p probe at room temperature for 2 h. The lysate was then incubated with pre-coated M-280 streptavidin magnetic beads (Sigma-Aldrich) for 4 h. The bound RNA was further purified by TRIzol, and then detected by qRT-PCR for H19 enrichment.

Statistical analysis

Statistical analysis was performed by SPSS 17.0 software (SPSS, Inc., Chicago, IL, USA).

Data were showed as the mean \pm standard deviation (SD) of three independent experiments. Differences between two groups was evaluated using unpaired Student's t-test and differences among multiple groups was assessed with one-way analysis of variance (ANOVA). A *P* value <0.05 was considered to be statistically significant.

Results

Morphological observation and identification of BMSCs and BMSCs-exos

BMSCs showed uniform morphology and spindle-shaped appearance (Figure 1A). Subsequently, BMSCs-derived exosomes (BMSCs-exos) were isolated and purified, and identified by TEM and western blot. As shown in Figure 1B and 1C, the results showed that BMSCs-exos were successfully detached and purified from the culture medium of BMSCs. Moreover, the enrichment of CD63, CD9, and CD81 on the surface of exosomes was detected by western blot assay (Figure 1D). These results indicated

that the BMSCs-exos obtained meet recognized standards.

BMSCs-exos attenuated LPS-induced M1 polarization and inflammatory response in BV-2 cells

To evaluate the effect of BMSCs-exos on the phenotype of LPS-stimulated BV-2 cells, qRT-PCR was utilized to measure the mRNA levels of M2 markers CD206, IL-10, and Arg-1 (**Figure 2A**), and M1 markers iNOS, CD86, and TNF- α (**Figure 2B**). As shown in **Figure 2A** and **2B**, LPS stimulation could down-regulate the levels of CD206, IL-10, and Arg-1 mRNA, whereas up-regulate the levels of iNOS, CD86, and TNF- α mRNA. In contrast, BMSCs-derived exosomes could inhibit the levels of iNOS, CD86, and TNF- α mRNA, while promote the expression of CD206, IL-10 and Arg-1 mRNA in LPS-stimulated BV-2 cells. Simultaneously, BMSCs-derived exosomes inhibited the secretion of pro-inflammatory factors (including IL-1 β , IL-6, and TNF- α) caused by LPS, while increased the level of inflammation inhibitory factor (IL-10) in BV-2 cells (**Figure 2C-F**). These data suggested that BMSCs-exos inhibited M1 polarization in LPS-stimulated BV-2 cells, meanwhile inhibited the neuroinflammation in LPS-activated BV-2.

BMSCs-exos inhibited neuronal apoptosis in HT22 cells following LPS stimulation

As shown in **Figure 3A**, a significant cell viability reduction of HT22 cells induced by LPS was noticed. However, BMSCs-exos treatment could resist the cytotoxicity induced by LPS in HT22 cells. The results of DNA fragmentation also showed that BMSCs-exos treatment reduced the apoptosis of HT22 cells induced by LPS (**Figure 3B**). Additionally, the increase in cell apoptosis rate and caspase-3 activity induced by LPS stimulation could be blocked by BMSCs-exos in a dose-dependent manner (**Figure 3C** and **3D**). These data revealed that BMSCs-exos could prevent LPS-induced neuronal apoptosis in HT22 hippocampal cells.

BMSCs-exosomal lncRNA H19 enhanced the effects of exosomes on BV-2 cells following LPS stimulation

To ascertain whether pcDNA-H19 could be packaged into exosomes, we transfected pcDNA-H19 or pcDNA into BMSCs. At 48 h after

transfection, BMSCs-exos were isolated and purified. As a result, the expression of H19 in BMSCs transfected with pcDNA-H19 was significantly increased compared with that transfected with pcDNA (**Figure 4A**). Meanwhile, pcDNA-H19-exos also showed enhanced expression of H19 (**Figure 4B**).

To determine whether BMSCs-exos successfully delivered H19 to BV-2 cells, BMSCs-exos carrying pcDNA-H19 (pcDNA-H19-exos) or pcDNA (pcDNA-exos) was co-cultured with BV-2. qRT-PCR showed that the H19 expression was increased in BV-2 cells co-cultured with pcDNA-H19-exos (**Figure 4C**).

Next, we explored whether BMSCs-exosomal H19 affects the polarization and neuroinflammation of LPS-stimulated BV-2 cells. pcDNA-H19-exos was co-cultured with BV-2, and then BV-2 was exposed to LPS. qRT-PCR revealed that co-culture of BV-2 cells with pcDNA-H19-exos enhanced the promotive effects of BMSCs-exos on the M2 polarization and the inhibition of M1 polarization in LPS-stimulated BV-2 cells, indicated by increased CD206, IL-10, and Arg-1 mRNA levels (**Figure 4D**), and reduced iNOS, CD86, and TNF- α mRNA levels (**Figure 4E**). Similarly, co-culture of BV-2 cells with pcDNA-H19-exos improved the anti-inflammatory effect of BMSCs-exos in LPS-stimulated BV-2 cells, which was manifested in inhibiting the secretion of IL-1 β , IL-6, and TNF- α , and increasing the content of IL-10 (**Figure 4F-I**). Therefore, BMSCs-exos inhibited the M1 polarization and neuroinflammation of LPS-stimulated BV-2 cells by transferring BMSCs-derived exosomal H19.

BMSCs-exosomal lncRNA H19 enhanced the neuroprotective effect of exosomes on HT22 cells treated with LPS

Next, we analyzed whether BMSCs-exosomal H19 treatment enhanced the neuroprotective effect of BMSCs-exos in HT22 cells treated with LPS. As expected, pcDNA-H19-exos treatment can enhance the effect of BMSCs-exos on the viability of HT22 cells induced by LPS (**Figure 5A**). Moreover, pcDNA-H19-exos enhanced the inhibitory effect of BMSCs-exos on apoptosis induced by LPS in HT22 cells, as indicated by the reduction of DNA fragmentation (**Figure 5B**), caspase-3 activity (**Figure 5C**), and apoptosis rate (**Figure 5D**).

MSCs-secreted exosomal H19 mitigates neuroinflammation

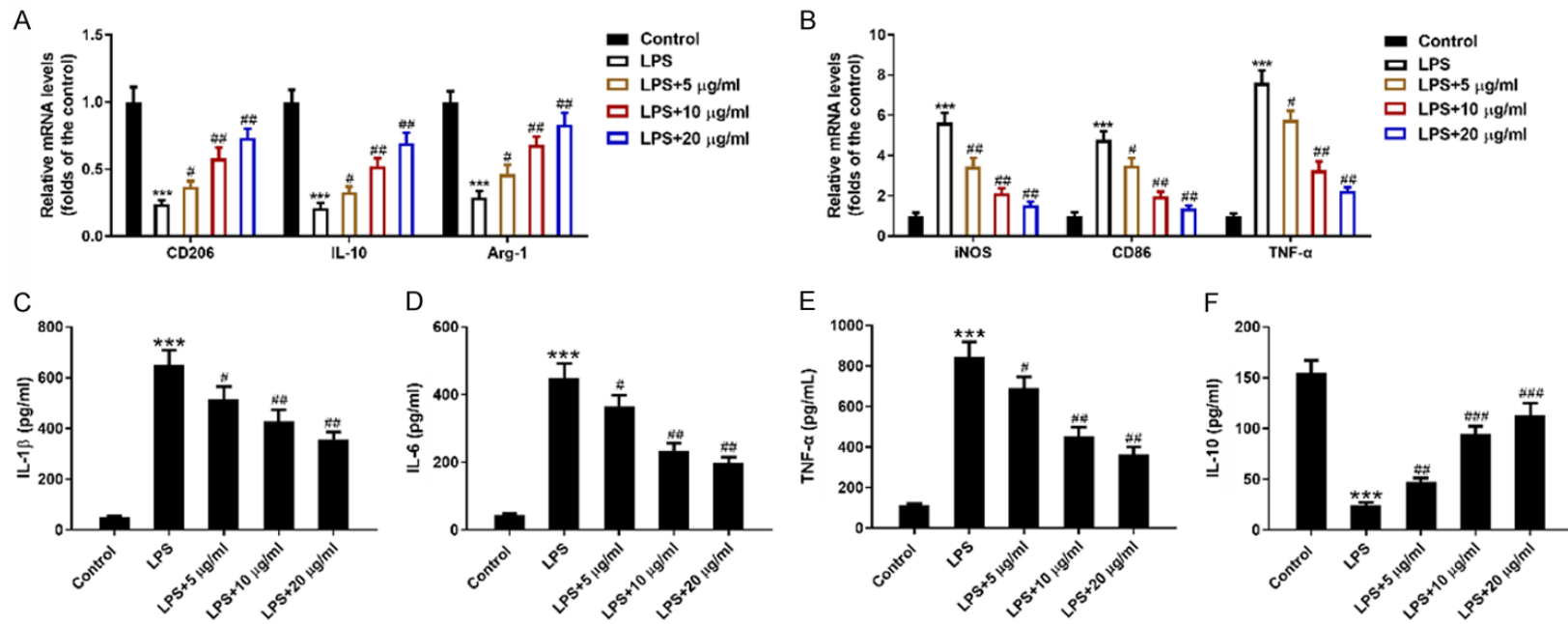


Figure 2. BMSCs-exos attenuated LPS-induced M1 polarization and inflammatory response in BV-2 cells. The mRNA levels of M2 markers (CD206, IL-10, and Arg-1) and M1 markers (iNOS, CD86, and TNF- α) (A and B) were detected by qRT-PCR. The contents of IL-1 β (C), IL-6 (D), TNF- α (E), and IL-10 (F) in the cell supernatant were detected by ELISA. *** P <0.001 vs the control group; # P <0.05, ## P <0.01, ### P <0.001 vs the LPS group.

MSCs-secreted exosomal H19 mitigates neuroinflammation

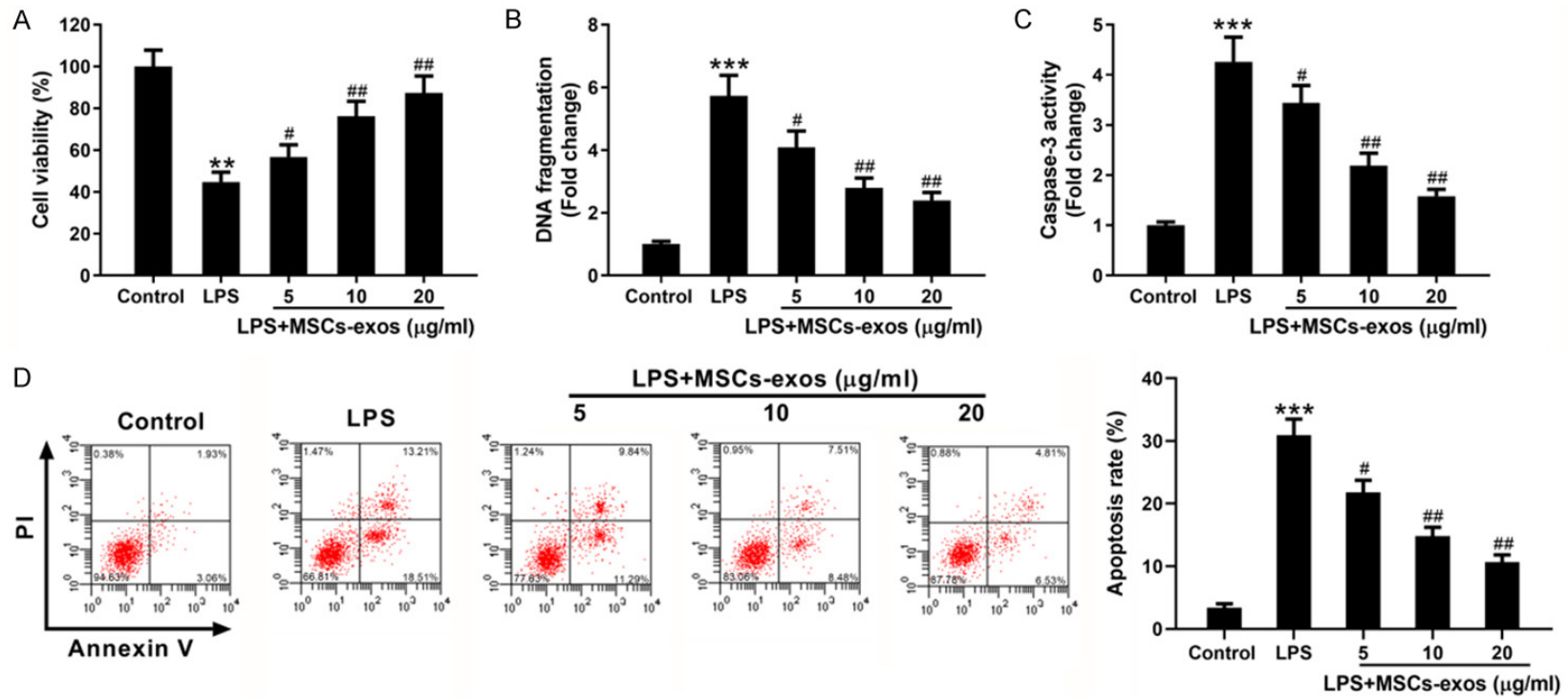


Figure 3. BMSCs-exos inhibited neuronal apoptosis in HT22 cells following LPS stimulation. HT22 cells were exposed to LPS for 12 h, and then incubated with BMSCs-exos for 48 h. A. Cell viability of HT22 cells was measured by CCK-8 assay. B. Cellular DNA fragmentation was analyzed by ELISA assay. C. Caspase-3 activity was measured by caspase-3 assay kit. D. Cell apoptosis rate was measured by flow cytometry. ** $P < 0.01$ and *** $P < 0.001$ vs the control group; # $P < 0.05$, ## $P < 0.01$ vs the LPS group.

MSCs-secreted exosomal H19 mitigates neuroinflammation

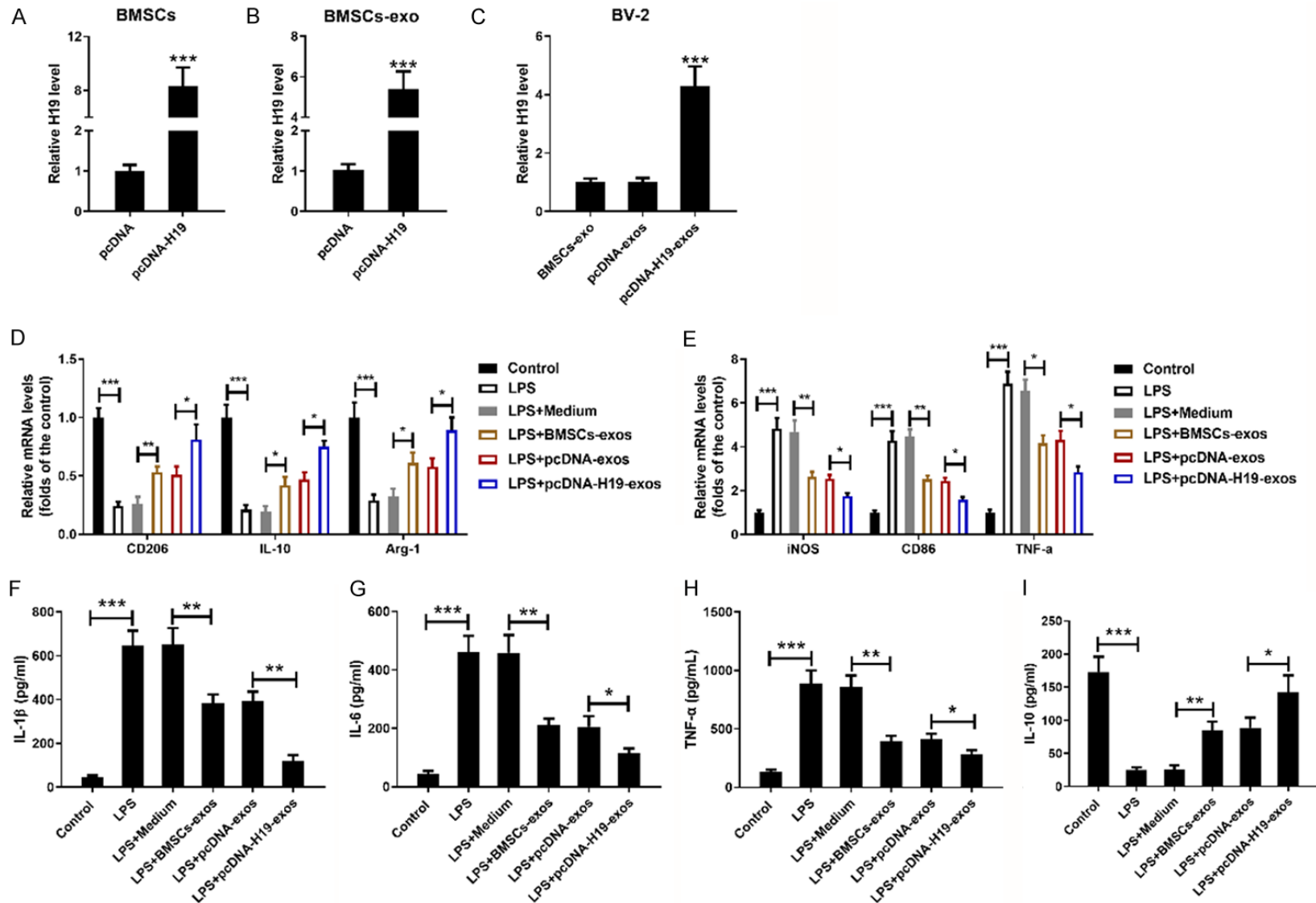


Figure 4. BMSCs-exosomal lncRNA H19 enhanced the effects of exosomes on BV-2 microglia following LPS stimulation. pcDNA-H19 or pcDNA was transfected into BMSCs. At 48 h after transfection, BMSCs-exos were separated and purified. qRT-PCR was used to detect the level of H19 in BMSCs (A) and BMSCs-exos (B). BMSCs-exos carrying pcDNA-H19 (pcDNA-H19-exos) or pcDNA (pcDNA-exos) were co-cultured with BV-2. (C) The level of H19 in BV-2 cells was detected using qRT-PCR. The mRNA levels of M2 markers (CD206, IL-10, and Arg-1), and M1 markers (iNOS, CD86, and TNF- α) were detected by qRT-PCR (D and E). The contents of IL-1 β (F), IL-6 (G), TNF- α (H), and IL-10 (I) in the cell supernatant were detected by ELISA. ** $P < 0.01$, *** $P < 0.001$.

MSCs-secreted exosomal H19 mitigates neuroinflammation

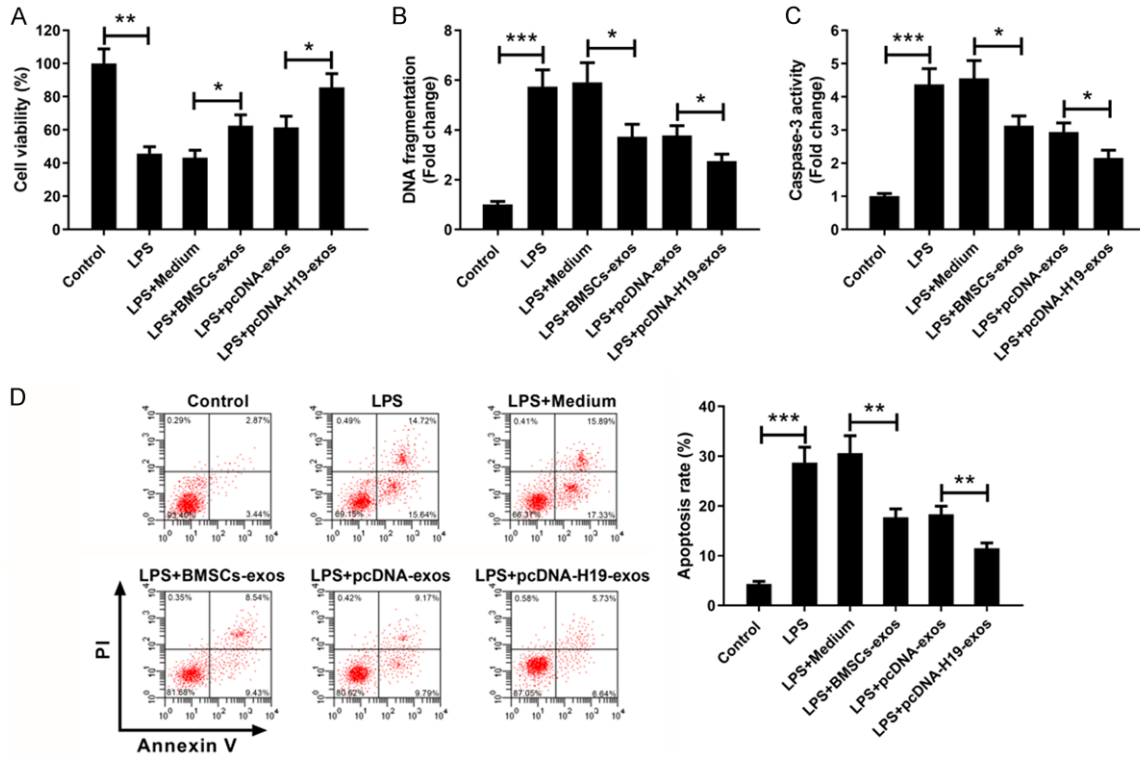


Figure 5. BMSCs-exosomal lncRNA H19 enhanced the neuroprotective effect of exosomes on HT22 cells treated with LPS. A. Cell viability of HT22 cells was measured by CCK-8 assay. B. Cellular DNA fragmentation was analyzed by ELISA assay. C. Caspase-3 activity was measured by caspase-3 assay kit. D. Cell apoptosis rate was measured by flow cytometry. ** $P < 0.01$, *** $P < 0.001$.

lncRNA H19 targeted miR-29b-3p

We next investigated the potential molecular target of lncRNA H19. Starbase predicted that miR-29b-3p and H19 had complementary sequences (**Figure 6A**). Subsequently, a luciferase activity was measured to assess the relationship between H19 and miR-29b-3p. H19-WT and H19-MUT luciferase reporter vectors were constructed and co-transfected with miR-29b-3p mimic or miR-NC into HT22 cells or BV-2 cells, respectively (**Figure 6B**). Luciferase reporter assay showed that miR-29b-3p mimic resulted in an obvious reduction of luciferase activity in H19-WT reporter compared with that in the miR-NC group, but it had no significant effect on H19-MUT reporter in HT22 cells and BV-2 cells (**Figure 6B**). Additionally, RNA pull down assay (**Figure 6C**) also confirmed the interaction between H19 and miR-29b-3p. Moreover, pcDNA-H19 or si-H19 were transfected into HT22 cells, respectively. qRT-PCR results showed that pcDNA-H19 transfection decreased miR-29b-3p expression, while si-H19 transfection increased miR-29b-3p expression in HT22 cells (**Figure 6D**).

miR-29b-3p overexpression reversed the effects of BMSCs-exosomal lncRNA H19 on LPS-stimulated BV-2 cells

To explore the role of H19/miR-29b-3p axis in BMSCs-exos-mediated attenuation of LPS-stimulated M1 polarization and inflammatory response, BV-2 cells were transfected with miR-29b-3p mimics, and then co-cultured with BMSCs-exos or pcDNA-H19-exos in the presence of LPS. miR-29b-3p mimics significantly reversed pcDNA-H19-exos-mediated M2 polarization induction (**Figure 7A**) and M1 polarization inhibition (**Figure 7B**) in LPS-stimulated BV-2 cells. Also, miR-29b-3p mimics significantly attenuated pcDNA-H19-exos-mediated anti-neuroinflammatory activity in LPS-stimulated BV-2 cells, as confirmed by ELISA (**Figure 7C-F**).

miR-29b-3p upregulation reversed the neuroprotective effect of BMSCs-exosomal lncRNA H19 on LPS-stimulated HT22 cells

miR-29b-3p mimics markedly attenuated pcDNA-H19-exos-mediated neuroprotective effects on LPS-stimulated HT22 cells, indicated by the

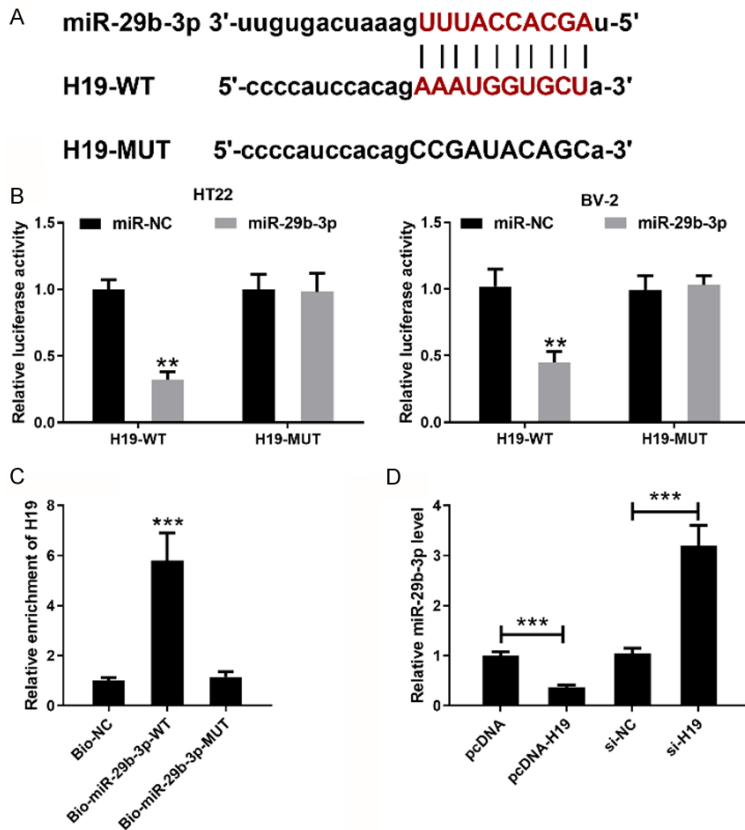


Figure 6. IncRNA H19 targeted miR-29b-3p. A. The putative binding site between IncRNA H19 and miR-29b-3p was shown. B. The effect of miR-29b-3p mimic on luciferase activity of H19 wild-type (H19-WT) or mutant (H19-MUT) luciferase reporter vector. C. The relationship between miR-29b-3p and H19 was confirmed by RNA pull down assay. D. The effect of H19 pcDNA or H19 siRNA on miR-29b-3p expression in HT22 cells. **P<0.01, ***P<0.001.

reduction of cell viability (**Figure 8A**) and the increase of DNA fragmentation (**Figure 8B**), caspase-3 activity (**Figure 8C**), and apoptosis rate (**Figure 8D**). The above data indicated that exosomal H19 derived from BMSCs implicated in BMSCs-exos-mediated neuroprotective effects via targeting miR-29b-3p (**Figure 9**).

Discussion

Neuroinflammation triggered by microglia is the key mechanism leading to secondary damage to the central nervous system [24]. Therapeutic targeting of inflammation is thought to be a promising approach for preventing neuronal injury [25]. Herein, we demonstrated that MSCs-exos improved the neuroinflammatory response induced by LPS in BV-2 cells and promoted the polarization of BV-2 cells from M1 to

M2. Additionally, MSCs-exos improved neuronal apoptosis induced by LPS in mouse hippocampal HT22 cells. More importantly, the anti-neuroinflammatory and neuroprotective effects of MSCs-exos in LPS-stimulated BV-2 cells were associated with exosomal lncRNA H19, which functioned as a miR-29b-3p sponge.

Microglia-mediated inflammation is associated with many neuropathological diseases, ranging from acute injury and chronic inflammation [26] to neurodegenerative disease [27]. There are two different phenotypes of microglia. M1 microglial cells exacerbate brain damage by releasing pro-inflammatory and neurotoxic factors, including IL-1 β , TNF- α , CD86, and iNOS. In contrast, M2 microglia cells secrete anti-inflammatory and neurotrophic mediators to repair brain injury, and their polarization markers include Arg-1, CD206, TGF- β , and IL-10 [28]. Compared with blocking the activation of microglia along, inhibiting the polarization of M1 microglia and promoting the polarization

of M2 microglia may be an attractive strategy against brain lesions [29]. To date, it has been proved that MSCs can act as effective immune regulatory cells and have therapeutic effects in the inflammatory and autoimmune diseases [30]. It has been confirmed in experimental models of cerebral ischemia and brain injury that MSCs from bone marrow and adipose tissues can improve experimental autoimmune encephalomyelitis and protect neurons from neuroinflammation damage [31-33]. Although the mechanism involved is largely unclear, it is worth noting that MSCs-exos seem to be able to regulate the activation of microglia [34]. Exosomes can serve as messengers between MSCs and differentiated cells [35]. So far, MSCs-exos alleviate acute brain injury by inhibiting microglia inflammation [15]. Consistent with previous reported anti-inflammatory

MSCs-secreted exosomal H19 mitigates neuroinflammation

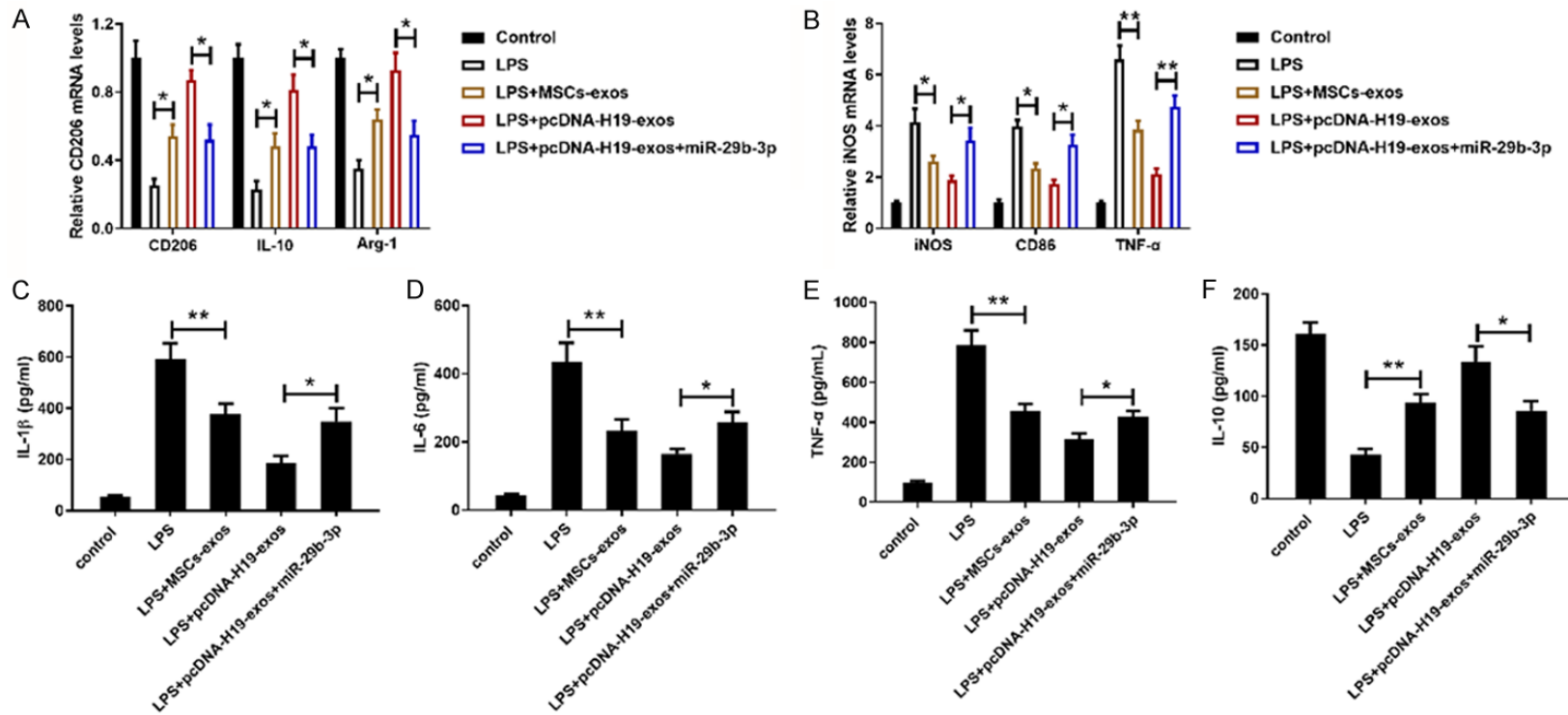


Figure 7. miR-29b-3p upregulation reversed the effects of BMSCs-exosomal lncRNA H19 on LPS-stimulated BV-2 cells. BV-2 cells transfected with miR-29b-3p mimics were treated with BMSCs-exos or pcDNA-H19-exos, and subsequently exposed to LPS. The mRNA levels of M2 markers (CD206, IL-10, and Arg-1) and M1 markers (iNOS, CD86, and TNF- α) were detected by qRT-PCR (A and B). The contents of IL-1 β (C), IL-6 (D), TNF- α (E), and IL-10 (F) in the cell supernatant were detected by ELISA. *P<0.05, **P<0.01.

MSCs-secreted exosomal H19 mitigates neuroinflammation

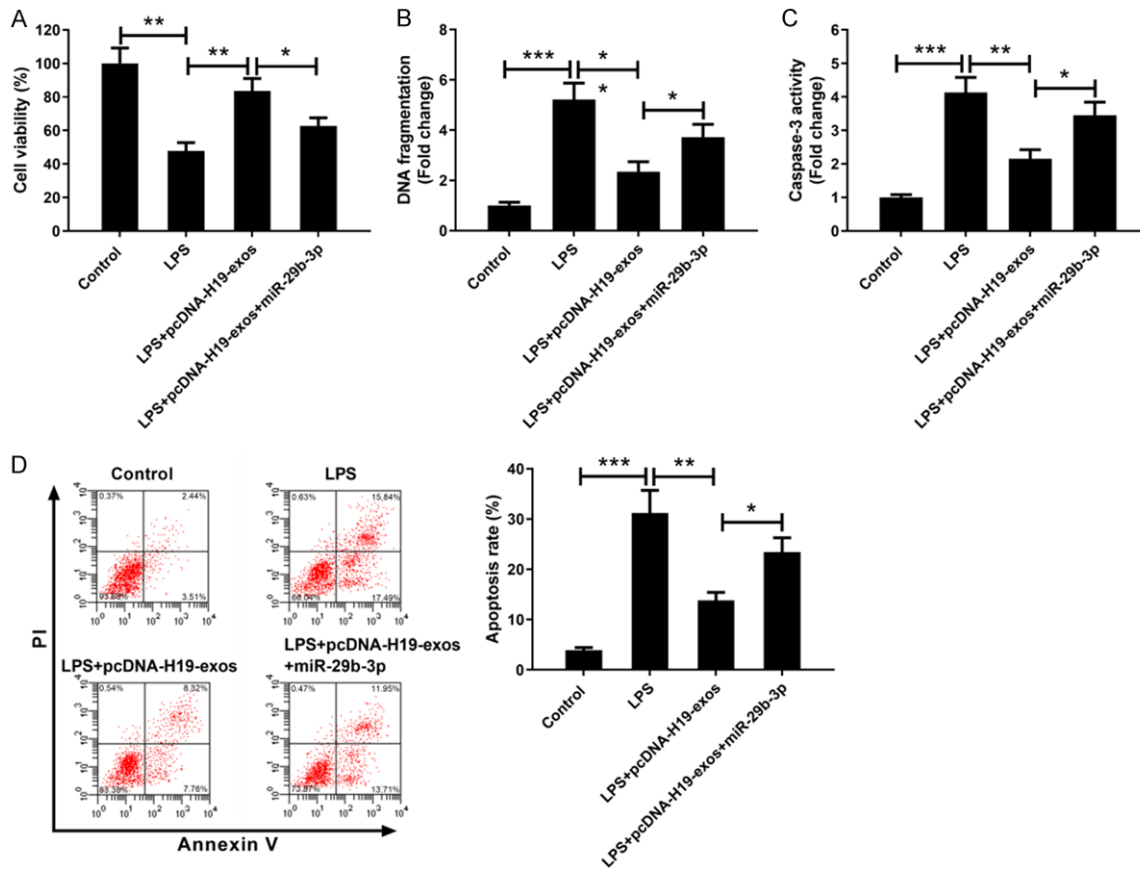


Figure 8. miR-29b-3p upregulation reversed the neuroprotective effect of BMSCs-exosomal H19 on HT22 cells treated with LPS. HT22 cells transfected with miR-29b-3p mimics were treated with BMSCs-exos or pcDNA-H19-exos, and subsequently exposed to LPS treatment. A. Cell viability of HT22 cells was measured by CCK-8 assay. B. Cellular DNA fragmentation was analyzed by ELISA assay. C. Caspase-3 activity was measured by caspase-3 assay kit. D. Cell apoptosis rate was measured by flow cytometry. ** $P < 0.01$, *** $P < 0.001$.

effects, we also observed that MSCs-exos attenuated LPS-induced inflammatory cytokine release by reducing M1 polarization of BV-2 microglia. Besides, BMSCs-exos could polarize BV-2 cells from M1 phenotype to anti-inflammatory M2 phenotype under LPS stimulation, thus promoting the production of anti-inflammatory cytokines. Moreover, we found that MSCs-exos also protected mouse hippocampal HT22 cells from LPS-stimulated injury. Therefore, BMSCs-exos could promote the LPS-stimulated microglia to M2 phenotypic polarization and protect against inflammation-induced neurotoxicity in HT22 cells.

RNA molecules (including mRNA, miRNA, circular RNA, and lncRNA) are highly enriched in exosomes [36, 37]. A large number of studies have proved that MSCs-exos are involved in the process of nerve repair by transporting functional

proteins and RNAs. For instance, Chen et al. [38] discovered that the increase of exosomal miR-233 is related to the occurrence, severity, and short-term prognosis of acute ischemic stroke, which can be used as a new biomarker for ischemic stroke. Wang et al. [39] proposed that adipose-derived MSCs-exosomal miR-21 enhances cardioprotection by inhibiting cardiomyocyte apoptosis via PTEN/AKT pathway. Tao et al. [40] showed that miR-140-5p derived from MSCs exosomes promotes proliferation and migration of rat chondrocytes to improve osteoarthritis. lncRNAs are no less than 200 bp in length and highly conserved non-protein-coding RNAs. Increasing evidence showed that lncRNAs are implicated in microglia activation [41, 42]. lncRNA H19 is a multiple functioned imprinted gene, which is located on human chromosome 11 [43]. H19 is upregulated in glioblastoma tissues and promotes the prolifer-

MSCs-secreted exosomal H19 mitigates neuroinflammation

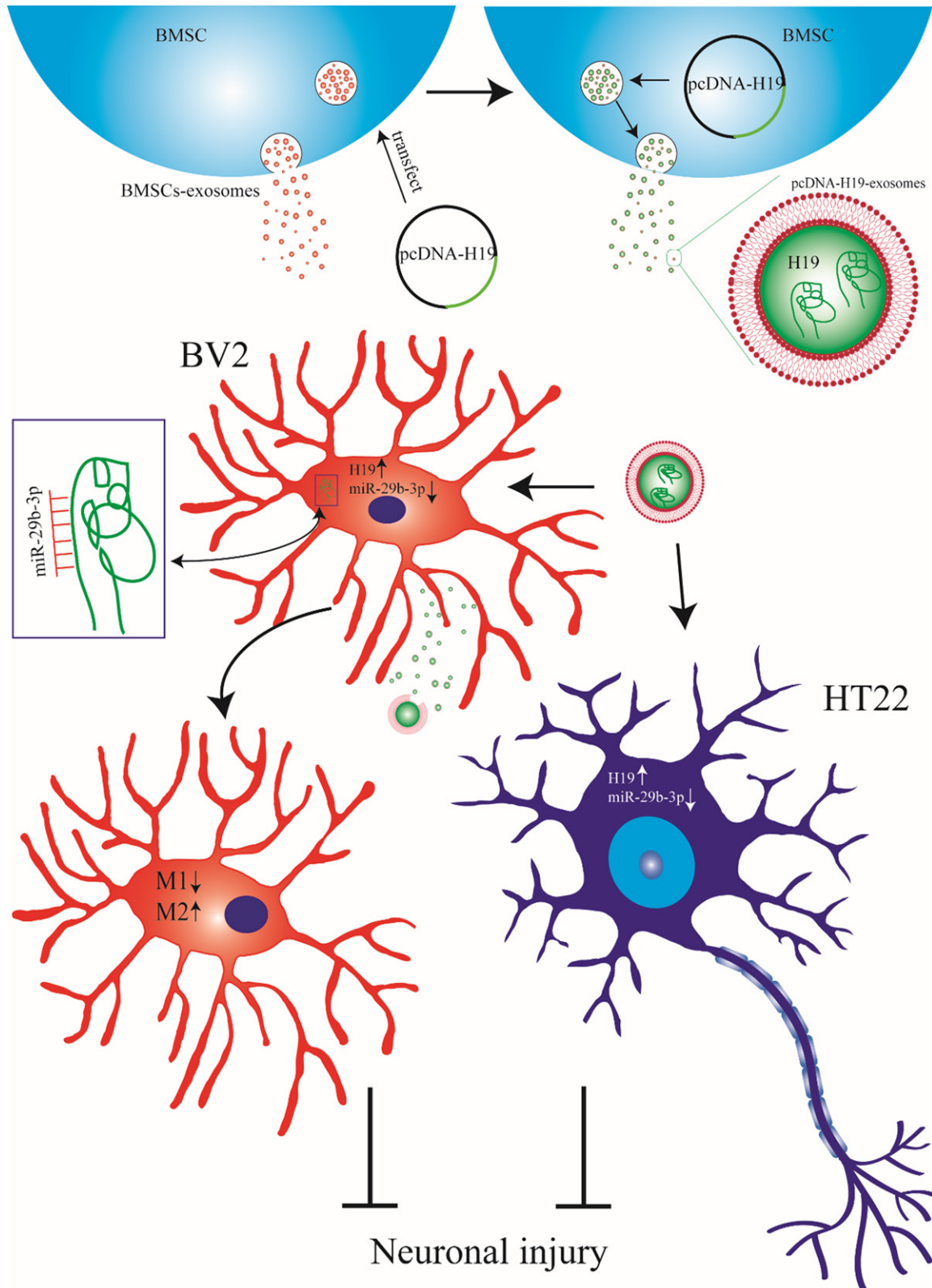


Figure 9. Schematic illustration of the mechanism underlying the effect of BMSCs-exosomal H19 on LPS-induced neuronal injury.

eration, migration, and invasion of glial cells [44, 45]. It has reported that H19 can promote the activation of hippocampal glial cells by regulating the JAK/STAT pathway [43]. Luo et al. [46] found that H19 inhibited the secretion of proinflammatory cytokines in retinal endothelial cells under high glucose condition. It is interesting to find that H19 transported by exosomes from MSCs enhance the invasion and migration, and inhibit apoptosis of trophoblast cells in preeclampsia [47]. Herein, we found H19 was enriched in BMSCs and BMSCs-exos. In addition, H19 could be delivered to BV-2 cells through BMSCs-secreted exosomes. More importantly, the upregulation of H19 in BMSCs-exos could enhance the effects of exosomes on LPS-stimulated microglia, including reducing the M1 polarization and increasing the M2 polarization of BV-2 microglia. Moreover, BMSCs-exosomal H19 enhanced the neuroprotective effect of BMSCs-exos on mouse hippocampal HT22 cells. These data suggested that exosomal H19 released by BMSCs could contribute to the anti-inflammatory and neuroprotective effects mediated by exosomes.

It is well known that lncRNAs isolate miRNAs from target mRNA by acting as competing endogenous RNA (ceRNA). For example, exosomal H19 acts as a ceRNA of miR-141 to activate the β -catenin pathway, thereby promoting the dryness and chemoresistance of colorectal cancer cells [48]. Using bioinformatics analysis, a predicted binding site for the miR-29b-3p on H19 was noticed. A recent study reported that miR-29b-3p expression was overexpressed in JEV-infected BV-2 cells, and miR-29b-3p knock-down could inhibit JEV-induced microglial activation and neuroinflammation [49]. Herein, we confirmed the targeting reaction between H19 and miR-29b-3p. In addition, the effects of BMSCs-derived exosomal H19 were correlated with its regulation of miR-29b-3p. BMSCs-derived exosomal H19 targeted miR-29b-3p to attenuate LPS-induced M1 polarization and inflammatory response in BV-2 cells, and inhibit neuronal apoptosis of HT22 cells following LPS stimulation.

In conclusion, our data indicated that BMSCs-exos mitigated LPS-induced M1 polarization and inflammation in BV-2 cells. Moreover, exosomal H19 attenuated injury of HT22 cells induced by LPS by targeting miR-29b-3p. The

present research will support novel insights for the treatment of inflammation-induced neurological diseases from the perspective of BMSCs-based treatment.

Acknowledgements

This study was funded by the National Natural Science Foundation of China (No. 81701532, No. 81601316), the Fund of Buchang-The First Affiliated Hospital of Xi'an Jiaotong University (BC2017-08), and Shaanxi Healthy Science Fund (No. 2018D055).

Disclosure of conflict of interest

None.

Address correspondence to: Lu Zong, Department of Obstetrics, The First Affiliated Hospital of Xi'an Jiaotong University, 277 Yanta West Road, Xi'an 710061, Shaanxi, China. Tel: +86-029-81220318; E-mail: catherazong@126.com; Yan Kang, Department of Obstetrics, Shandong Provincial Maternal and Child Health Care Hospital, Cheeloo College of Medicine, Shandong University, Ji'nan 250014, Shandong, China. Tel: +86-0531-68777266; E-mail: kangrecrx269@126.com

References

- [1] Peng CC, Chang JH, Lin HY, Cheng PJ and Su BH. Intrauterine inflammation, infection, or both (Triple I): a new concept for chorioamnionitis. *Pediatr Neonatol* 2018; 59: 231-237.
- [2] Bashiri A, Burstein E and Mazor M. Cerebral palsy and fetal inflammatory response syndrome: a review. *J Perinat Med* 2006; 34: 5-12.
- [3] Ginhoux F, Greter M, Leboeuf M, Nandi S, See P, Gokhan S, Mehler MF, Conway SJ, Ng LG, Stanley ER, Samokhvalov IM and Merad M. Fate mapping analysis reveals that adult microglia derive from primitive macrophages. *Science* 2010; 330: 841-845.
- [4] Lee JH, Wei ZZ, Cao W, Won S, Gu X, Winter M, Dix TA, Wei L and Yu SP. Regulation of therapeutic hypothermia on inflammatory cytokines, microglia polarization, migration and functional recovery after ischemic stroke in mice. *Neurobiol Dis* 2016; 96: 248-260.
- [5] Ślusarczyk J, Trojan E, Głombik K, Piotrowska A, Budziszewska B, Kubera M and Popiotek-Barczyk K. Targeting the NLRP3 inflammasome-related pathways via tianeptine treatment-suppressed microglia polarization to the

MSCs-secreted exosomal H19 mitigates neuroinflammation

- M1 phenotype in lipopolysaccharide-stimulated cultures. *Int J Mol Sci* 2018; 19: 1965.
- [6] Bok E, Chung YC, Kim KS, Baik HH, Shin WH and Jin BK. Modulation of M1/M2 polarization by capsaicin contributes to the survival of dopaminergic neurons in the lipopolysaccharide-lesioned substantia nigra in vivo. *Exp Mol Med* 2018; 50: 1-14.
- [7] Kim H, Lee MJ, Bae EH, Ryu JS, Kaur G, Kim HJ, Kim JY, Barreda H, Jung SY, Choi JM, Shigemoto-Kuroda T, Oh JY and Lee RH. Comprehensive molecular profiles of functionally effective MSC-derived extracellular vesicles in immunomodulation. *Mol Ther* 2020; 28: 1628-1644.
- [8] Liu L and He YR. Enhanced effect of IL-1 β -activated adipose-derived MSCs (ADMSCs) on repair of intestinal ischemia-reperfusion injury via COX-2-PGE(2) signaling. *Stem Cells Int* 2020; 2020: 2803747.
- [9] Diomede F, Marconi GD, Fonticoli L, Pizzicanello J, Merciaro I, Bramanti P, Mazzon E and Trubiani O. Functional relationship between osteogenesis and angiogenesis in tissue regeneration. *Int J Mol Sci* 2020; 21: 3242.
- [10] Li L, Zhang Y, Mu J, Chen J, Zhang C, Cao H and Gao J. Transplantation of human mesenchymal stem-cell-derived exosomes immobilized in an adhesive hydrogel for effective treatment of spinal cord injury. *Nano Lett* 2020; 20: 4298-4305.
- [11] Krämer-Albers EM and Hill AF. Extracellular vesicles: interneural shuttles of complex messages. *Curr Opin Neurobiol* 2016; 39: 101-7.
- [12] Hartmann A, Muth C, Dabrowski O, Krasmann S and Glatzel M. Exosomes and the prion protein: more than one truth. *Front Neurosci* 2017; 11: 194.
- [13] Lo Sicco C, Reverberi D, Balbi C, Ulivi V, Principi E, Pascucci L, Becherini P, Bosco MC, Varesio L, Franzin C, Pozzobon M, Cancedda R and Tasso R. Mesenchymal stem cell-derived extracellular vesicles as mediators of anti-inflammatory effects: endorsement of macrophage polarization. *Stem Cells Transl Med* 2017; 6: 1018-1028.
- [14] Li G, Xiao L, Qin H, Zhuang Q, Zhang W, Liu L, Di C and Zhang Y. Exosomes-carried microRNA-26b-5p regulates microglia M1 polarization after cerebral ischemia/reperfusion. *Cell Cycle* 2020; 19: 1022-1035.
- [15] Zhao Y, Gan Y, Xu G, Yin G and Liu D. MSCs-derived exosomes attenuate acute brain injury and inhibit microglial inflammation by reversing CysLT2R-ERK1/2 mediated microglia M1 polarization. *Neurochem Res* 2020; 45: 1180-1190.
- [16] Qin Y, Sun R, Wu C, Wang L and Zhang C. Exosome: a novel approach to stimulate bone regeneration through regulation of osteogenesis and angiogenesis. *Int J Mol Sci* 2016; 17: 712.
- [17] Zhang C, Yang X, Qi Q, Gao Y, Wei Q and Han S. lncRNA-HEIH in serum and exosomes as a potential biomarker in the HCV-related hepatocellular carcinoma. *Cancer Biomark* 2018; 21: 651-659.
- [18] Xue M, Chen W, Xiang A, Wang R, Chen H, Pan J, Pang H, An H, Wang X, Hou H and Li X. Hypoxic exosomes facilitate bladder tumor growth and development through transferring long non-coding RNA-UCA1. *Mol Cancer* 2017; 16: 143.
- [19] Işın M, Uysaler E, Özgür E, Köseoğlu H, Şanlı Ö, Yücel ÖB, Gezer U and Dalay N. Exosomal lncRNA-p21 levels may help to distinguish prostate cancer from benign disease. *Front Genet* 2015; 6: 168.
- [20] Tao Y, Tang Y, Yang Z, Wu F, Wang L, Yang L, Lei L, Jing Y, Jiang X, Jin H, Bai Y and Zhang L. Exploration of serum exosomal lncRNA TBILA and AGAP2-AS1 as promising biomarkers for diagnosis of non-small cell lung cancer. *Int J Biol Sci* 2020; 16: 471-482.
- [21] Chen L, Yang W, Guo Y, Chen W, Zheng P, Zeng J and Tong W. Exosomal lncRNA GAS5 regulates the apoptosis of macrophages and vascular endothelial cells in atherosclerosis. *PLoS One* 2017; 12: e0185406.
- [22] Liu Y, Zou R, Wang Z, Wen C, Zhang F and Lin F. Exosomal KLF3-AS1 from hMSCs promoted cartilage repair and chondrocyte proliferation in osteoarthritis. *Biochem J* 2018; 475: 3629-3638.
- [23] Juknat A, Gao F, Coppola G, Vogel Z and Kozela E. miRNA expression profiles and molecular networks in resting and LPS-activated BV-2 microglia-Effect of cannabinoids. *PLoS One* 2019; 14: e0212039.
- [24] Marsters CM, Nesan D, Far R, Klenin N, Pittman QJ and Kurrasch DM. Embryonic microglia influence developing hypothalamic glial populations. *J Neuroinflammation* 2020; 17: 146.
- [25] Baune BT. Inflammation and neurodegenerative disorders: is there still hope for therapeutic intervention? *Curr Opin Psychiatry* 2015; 28: 148-154.
- [26] Napoli I and Neumann H. Protective effects of microglia in multiple sclerosis. *Exp Neurol* 2010; 225: 24-28.
- [27] McLarnon JG. Consideration of a pharmacological combinatorial approach to inhibit chronic inflammation in Alzheimer's disease. *Curr Alzheimer Res* 2019; 16: 1007-1017.
- [28] Brifault C, Gras M, Liot D, May V, Vaudry D and Wurtz O. Delayed pituitary adenylate cyclase-activating polypeptide delivery after brain stroke improves functional recovery by induc-

- ing m2 microglia/macrophage polarization. *Stroke* 2015; 46: 520-528.
- [29] Colton CA. Heterogeneity of microglial activation in the innate immune response in the brain. *J Neuroimmune Pharmacol* 2009; 4: 399-418.
- [30] Phinney DG and Prockop DJ. Concise review: mesenchymal stem/multipotent stromal cells: the state of transdifferentiation and modes of tissue repair—current views. *Stem Cells* 2007; 25: 2896-2902.
- [31] Constantin G, Marconi S, Rossi B, Angiari S, Calderan L, Anghileri E, Gini B, Bach SD, Martinello M, Bifari F, Galiè M, Turano E, Budui S, Sbarbati A, Krampera M and Bonetti B. Adipose-derived mesenchymal stem cells ameliorate chronic experimental autoimmune encephalomyelitis. *Stem Cells* 2009; 27: 2624-2635.
- [32] Uccelli A, Benvenuto F, Laroni A and Giunti D. Neuroprotective features of mesenchymal stem cells. *Best Pract Res Clin Haematol* 2011; 24: 59-64.
- [33] Zappia E, Casazza S, Pedemonte E, Benvenuto F, Bonanni I, Gerdoni E, Giunti D, Ceravolo A, Cazzanti F, Frassoni F, Mancardi G and Uccelli A. Mesenchymal stem cells ameliorate experimental autoimmune encephalomyelitis inducing T-cell anergy. *Blood* 2005; 106: 1755-1761.
- [34] Neubrand VE, Pedreño M, Caro M, Forte-Lago I, Delgado M and Gonzalez-Rey E. Mesenchymal stem cells induce the ramification of microglia via the small RhoGTPases Cdc42 and Rac1. *Glia* 2014; 62: 1932-1942.
- [35] Chang YH, Wu KC, Harn HJ, Lin SZ and Ding DC. Exosomes and stem cells in degenerative disease diagnosis and therapy. *Cell Transplant* 2018; 27: 349-363.
- [36] Mateescu B, Kowal EJ, van Balkom BW, Bartel S, Bhattacharyya SN, Buzás EI, Buck AH, de Candia P, Chow FW, Das S, Driedonks TA, Fernández-Messina L, Haderk F, Hill AF, Jones JC, Van Keuren-Jensen KR, Lai CP, Lässer C, Liegro ID, Lunavat TR, Lorenowicz MJ, Maas SL, Mäger I, Mittelbrunn M, Momma S, Mukherjee K, Nawaz M, Pegtel DM, Pfaffl MW, Schiffelers RM, Tahara H, Théry C, Tosar JP, Wauben MH, Witwer KW and Nolte-t Hoen EN. Obstacles and opportunities in the functional analysis of extracellular vesicle RNA - an ISEV position paper. *J Extracell Vesicles* 2017; 6: 1286095.
- [37] Ramirez MI, Amorim MG, Gadelha C, Milic I, Welsh JA, Freitas VM, Nawaz M, Akbar N, Couch Y, Makin L, Cooke F, Vettore AL, Batista PX, Freezor R, Pezuk JA, Rosa-Fernandes L, Carreira ACO, Devitt A, Jacobs L, Silva IT, Coakley G, Nunes DN, Carter D, Palmisano G and Dias-Neto E. Technical challenges of working with extracellular vesicles. *Nanoscale* 2018; 10: 881-906.
- [38] Chen Y, Song Y, Huang J, Qu M, Zhang Y, Geng J, Zhang Z, Liu J and Yang GY. Increased circulating exosomal miRNA-223 is associated with acute ischemic stroke. *Front Neurol* 2017; 8: 57.
- [39] Wang K, Jiang Z, Webster KA, Chen J, Hu H, Zhou Y, Zhao J, Wang L, Wang Y, Zhong Z, Ni C, Li Q, Xiang C, Zhang L, Wu R, Zhu W, Yu H, Hu X and Wang J. Enhanced cardioprotection by human endometrium mesenchymal stem cells driven by exosomal microRNA-21. *Stem Cells Transl Med* 2017; 6: 209-222.
- [40] Tao SC, Yuan T, Zhang YL, Yin WJ, Guo SC and Zhang CQ. Exosomes derived from miR-140-5p-overexpressing human synovial mesenchymal stem cells enhance cartilage tissue regeneration and prevent osteoarthritis of the knee in a rat model. *Theranostics* 2017; 7: 180-195.
- [41] Jiang ZS and Zhang JR. LncRNA SNHG5 enhances astrocytes and microglia viability via upregulating KLF4 in spinal cord injury. *Int J Biol Macromol* 2018; 120: 66-72.
- [42] Sun D, Yu Z, Fang X, Liu M, Pu Y, Shao Q, Wang D, Zhao X, Huang A, Xiang Z, Zhao C, Franklin RJ, Cao L and He C. LncRNA GAS5 inhibits microglial M2 polarization and exacerbates demyelination. *EMBO Rep* 2017; 18: 1801-1816.
- [43] Han CL, Ge M, Liu YP, Zhao XM, Wang KL, Chen N, Meng WJ, Hu W, Zhang JG, Li L and Meng FG. LncRNA H19 contributes to hippocampal glial cell activation via JAK/STAT signaling in a rat model of temporal lobe epilepsy. *J Neuroinflammation* 2018; 15: 103.
- [44] Jiang X, Yan Y, Hu M, Chen X, Wang Y, Dai Y, Wu D, Wang Y, Zhuang Z and Xia H. Increased level of H19 long noncoding RNA promotes invasion, angiogenesis, and stemness of glioblastoma cells. *J Neurosurg* 2016; 2016: 129-136.
- [45] Jia P, Cai H, Liu X, Chen J, Ma J, Wang P, Liu Y, Zheng J and Xue Y. Long non-coding RNA H19 regulates glioma angiogenesis and the biological behavior of glioma-associated endothelial cells by inhibiting microRNA-29a. *Cancer Lett* 2016; 381: 359-369.
- [46] Luo R, Xiao F, Wang P and Hu YX. lncRNA H19 sponging miR-93 to regulate inflammation in retinal epithelial cells under hyperglycemia via XBP1s. *Inflamm Res* 2020; 69: 255-265.
- [47] Chen Y, Ding H, Wei M, Zha W, Guan S, Liu N, Li Y, Tan Y, Wang Y and Wu F. MSC-secreted exosomal H19 promotes trophoblast cell invasion and migration by downregulating let-7b and

MSCs-secreted exosomal H19 mitigates neuroinflammation

- upregulating FOXO1. *Mol Ther Nucleic Acids* 2020; 19: 1237-1249.
- [48] Ren J, Ding L, Zhang D, Shi G, Xu Q, Shen S, Wang Y, Wang T and Hou Y. Carcinoma-associated fibroblasts promote the stemness and chemoresistance of colorectal cancer by transferring exosomal lncRNA H19. *Theranostics* 2018; 8: 3932-3948.
- [49] Jadhav VS, Krause KH and Singh SK. HIV-1 Tat C modulates NOX2 and NOX4 expressions through miR-17 in a human microglial cell line. *J Neurochem* 2014; 131: 803-815.